2025 SCEC Technical Report

SCEC Award #: 25154

Project Title: Joint Characterization of Transient Deformation and Repeating Earthquakes in California

PIs:
Junle Jiang (The University of Oklahoma, USA)
Taka'aki Taira (University of California, Berkeley, USA)

Project Period: February 1, 2025 – January 31, 2026

Proposal Category: Collaborative Research Project (Multiple Investigators / Institutions)

SCEC Science Milestones Addressed: A1-2, A3-5, B2-2, D1-1

Summary

Fault zones exhibit a spectrum of slip behavior, including wave-producing earthquake ruptures occurring over seconds to minutes and slower movements over longer timescales from hours to months or longer. California is a natural laboratory of diverse fault activities monitored by dense geophysical networks. Geodetic techniques measure ground displacement, crustal strain, or surface creep using ground- and space-based instruments, including strainmeters, creepmeters, GPS/GNSS (Global Positioning System/Global Navigation Satellite System), and InSAR (Interferometric Synthetic Aperture Radar) (Agnew, 1986; Bilham et al., 2004; Burgmann et al., 2000; Segall & Davis, 1997). Seismological observations illuminate detailed earthquakes and fault structures (Hauksson et al., 2012; Ross et al., 2019; Waldhauser & Ellsworth, 2000). In particular, characteristically repeating earthquakes (CRE) are seismic events that rupture the same fault areas and produce nearly identical waveforms in crustal faults and subduction zones, serving as potentially reliable indicators of fault slip (Nadeau & Johnson, 1998; Uchida & Bürgmann, 2019). The T_r-M_0 relation can be converted into a slip-moment relation, assuming a long-term fault slip rate, forming the basis for using CREs as creepmeters at seismogenic depths (Nadeau & Johnson, 1998; Nadeau & McEvilly, 2004). Hence, high-resolution geodesy and CREs estimates provide complementary measurements of transient deformation and fault slip.

Several fault segments in California are well known for their seismic and aseismic behaviors. The Parkfield segment of the San Andreas Fault (SAF) features an abundance of transient aseismic phenomena and CREs (Bakun et al., 2005; Nadeau & Johnson, 1998). The pre-, co-, and post-seismic phases of the 2004 M_w 6.0 Parkfield event are comprehensively studied using seismograms, high-rate GNSS, strainmeters, and creepmeters (Johanson et al., 2006; Langbein et al., 2006; Murray & Langbein, 2006). The spectrum of fault creep and seismicity extends along the Central San Andreas Fault (CSAF) (Bilham et al., 2004; Jolivet et al., 2015; Liu et al., 2022). Toward the south, fault creep or slow slip events were documented along the southernmost SAF (SSAF) (Lindsey et al., 2014; Tymofyeyeva et al., 2019), San Jacinto Fault (SJF) (Inbal et al., 2017; Shaddox et al., 2021), Superstition Hills fault (SHF) (M. Wei et al., 2009, 2015), and faults in the Salton Trough (Lohman & McGuire, 2007; S. Wei et al., 2015). CREs and seismicity were observed in most of these settings, but exhibited different behavior. Despite the increase in case studies, the relationship between transient aseismic faulting and coincident seismicity remains complex and challenging to interpret due to observational gaps and variability across geological settings.

In this SCEC project, we have compiled datasets and investigated a diverse range of transient deformation, surface creep, and fault slip, along with CREs in selected regions across California. Our study areas include major segments (SJB and Parkfield) of the San Andreas Fault, Superstition Hills Fault, San Jacinto Fault, and the Salton Sea. Building on geodetic data products from prior SCEC projects, we have analyzed geodetic observations of transient deformation (creepmeters, strainmeters, and GNSS) and CRE-based fault slip histories in some priority regions, determined the characteristic amplitudes and timescales of these transients, and evaluated cross-region variabilities, toward a systematic analysis of full datasets. To better characterize fault slip inferred from CREs, we have also updated the CRE catalog up to the end of 2025 in northern California faulting systems (Hayward, Parkfield). Our analysis reveals distinct temporal behaviors of aseismic transients attributed to (1) creeping vs seismogenic faults, (2) spontaneous, triggered, and postseismic modes, and (3) factors of source depths and instrumental apertures. These initial results highlight the diversity and complexity of seismic-aseismic faulting and may aid future validations of physical models of faulting and inform the development of effective rheology laws and earthquake forecasts.

Results: Transient Deformation and Characteristics

Over the duration of the project, we have compiled and analyzed geodetic and seismic observations over periods of interest since 1998–2000 at selected sites across California (Figure 1). PI Jiang and a graduate student have processed geodetic datasets; PI Taira has improved RE catalogs for major faults. Using a subset of compiled datasets, we have characterized deformation transients in terms of effective amplitudes and timescales using parametric function fits.

Geodetic and Seismic Datasets. We have examined multi-sensor datasets for the regions:

1) CSAF, Parkfield – Subdaily and daily GNSS displacements for postseismic signals of the 2003 M6.5 San Simeon and 2004 M6 Parkfield earthquake (Langbein et al., 2006; Murray & Langbein, 2006) and potential short-term transients in 2012, 2016, and 2017 (Michel et al., 2022). In addition to our GNSS and creepmeter datasets (Jiang et al., 2021), we have compiled creepmeter and borehole strainmeter records (Johnston et al., 2006; Langbein et al., 2024), along with a CRE catalog by Taira.
2) CSAF, San Juan Bautista – Creepmeter records for episodic creep events (Gittins & Hawthorne, 2022, 2024; Langbein et al., 2024) and borehole strainmeter records following 5 M4+ events since a 1998 M5.1 earthquake (Hawthorne et al., 2016), and CRE/NCSN catalogs (Waldhauser & Ellsworth, 2000).
3) SJF near Anza – Strainmeter records for spontaneous and triggered transients, along with catalogs of near-repeating earthquakes (NRE) (Inbal et al., 2017; Ross et al., 2017; Shaddox et al., 2021) and a few CREs identified by Taira.
4) SSAF & SHF – Creepmeter records for spontaneous or triggered creep on shallow SSAF (Lindsey et al., 2014; Tymofyeyeva et al., 2019) and SHF in 2006, 2010, 2017, and 2023 (Jiang & Lohman, 2021; Materna et al., 2024; Vavra et al., 2024; M. Wei et al., 2015). Few CREs are identified in this region.
5) Faults in Salton Trough – InSAR and GNSS observations for aseismic deformation associated with M~5 earthquake swarms in this region in 2005, 2012, 2020, and 2021 (Lohman & McGuire, 2007; Materna et al., 2022; Sirorattanakul et al., 2022; S. Wei et al., 2015). Few CREs are identified in this region.

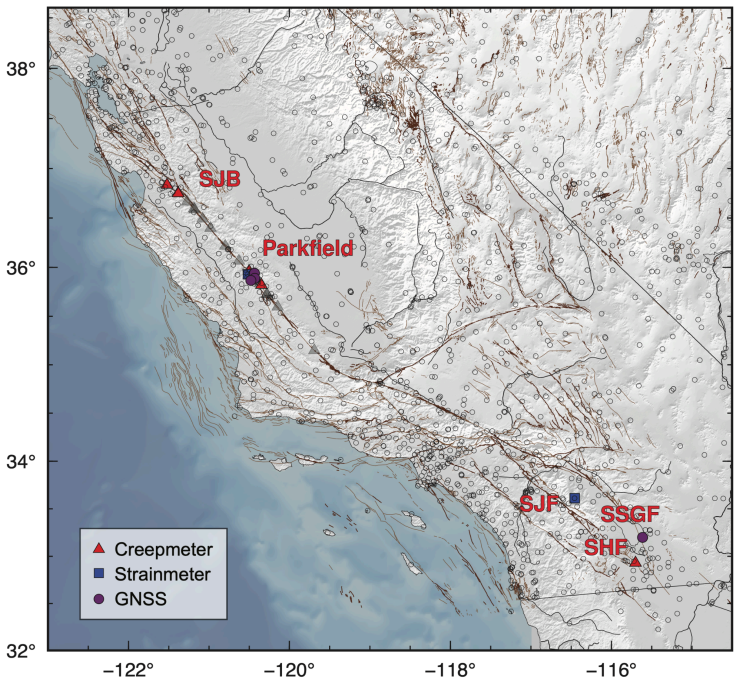

Figure 1. Geodetic networks across California. Locations of creepmeter (triangles), strainmeter (squares), and GNSS stations (circles) are marked. Data are selected from stations in colors. Brown lines mark quaternary fault traces.

Geodetic Trasient Characteristics

Most transient geodetic signals have rates that decay over time since rapid fault slip initiation. To guide a systematic investigation, we begin with a subset of representative cases—including different forms of transient signals associated with different areas, depths, and causes—and fit logarithmic and exponential decay functions to time-series data for GNSS displacements, strain, and creep, similar to postseismic studies of afterslip or viscoelastic relaxation

(Langbein et al., 2006; Savage et al., 2005). Because these observations are distant or local measures of a complex finite source, the effective (logarithmic) characteristic timescales, T_c, estimated at each station may vary in space, especially in early transient periods, pointing to evolving source location or size, and generally depend on the considered time window, as demonstrated for Parkfield (Jiang et al., 2021). Time-dependent geodetic source inversions will directly constrain source properties, an important consideration in future.

Our preliminary results are:

1) Transient creep observations. The high temporal resolutions of creepmeter records allow us to characterize the complete history of fault creep transients at the Earth's surface. We cross-examine transient creep events on primarily creeping faults (SJB and Parkfield), on shallow creeping areas above the seismogenic zone (SHF), and afterslip following a major earthquake (2004 M6 Parkfield) (Figure 2). At each location of small transient events (CWN, XGH, CoSH), their slip amplitudes over 3–7 days reach the order of 1–10 mm, while their effective timescales vary over ~3 orders of magnitude within 10^{-3}–10 days, with longer timescales for larger-amplitude events. While CWN and XGH share similar characteristics, coSH has smaller timescales for spontaneous creep events and even smaller values for dynamically triggered events. This indicates different characteristics of creep events on a primarily creeping vs seismogenic/locked fault. Furthermore, comparing these cases with post-2004 Parkfield demonstrates that the latter have comparable, yet larger characteristic timescales (1–10 days) and higher slip amplitudes. One caveat here is that these estimates are confined to the surface fault behavior and can change substantially with depth, depending on how creep events propagate (Bilham & Behr, 1992; Tymofyeyeva et al., 2019; M. Wei et al., 2015). These early results motivate more detailed kinematic modeling and characterization that can inform dynamic constitutive models.

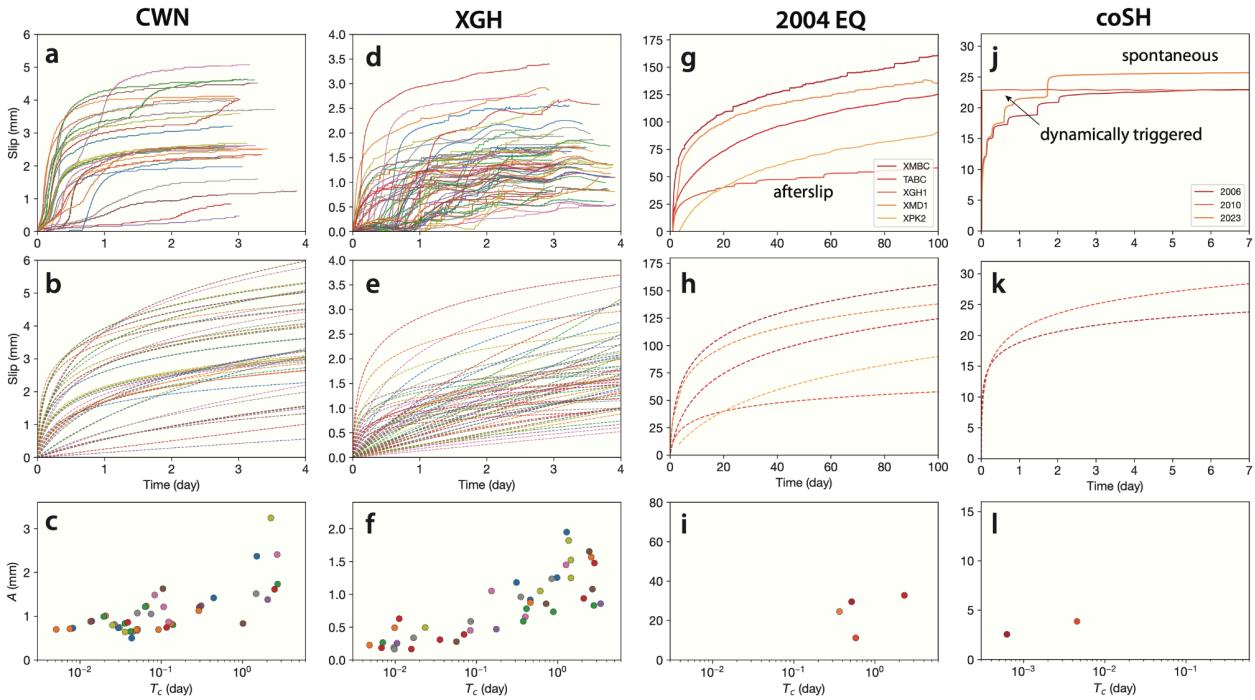

Figure 2. Characterizing transient creep events at different sites. (a, d, j) Fault slip histories during transient creep events at CWN (SJB), XGH (Parkfield), and coSH (SHF) (Gittins & Hawthorne, 2022, 2024; Langbein et al., 2024). (g) Postseismic creep after the 2004 Parkfield earthquake at different creepmeters (Jiang et al., 2021). (b, e, h, k) Logarithmic function fits of transient slip. (c, f, i, l) Effective amplitude vs timescale for each record. Colors indicate different (a, d, j) creep events or (g) creepmeters, consistent across three rows.

2) GNSS and strain observations. Similar comparative analysis of other transient signals recorded by GNSS and strainmeters further demonstrates variable fault behavior, with caveats for different data types (Figure 3). High-resolution GNSS data at Parkfield documents robust, very early postseismic signals (Figure 3a–b), with effective timescales ranging from 0.1–10 days, consistent with (Jiang et al., 2021). These estimates are smaller than those inferred from creepmeter records (Figure 2g). This likely reflects the different apertures of these instruments—dense GNSS network captures deep slip evolution, and creepmeters are only sensitive to fault slip at the surface—highlighting the need for more detailed models. GNSS displacements for transient slip and swarms in the Salton Sea exhibit much weaker amplitudes but comparable timescales (Figure 3c–d). The interpretation is, however, challenged by the sparse, noisy GNSS in this region and requires integration of InSAR/models. Strain transients at SJF are robust with moderate noise; the interpreted timescales are comparable but require further verification.

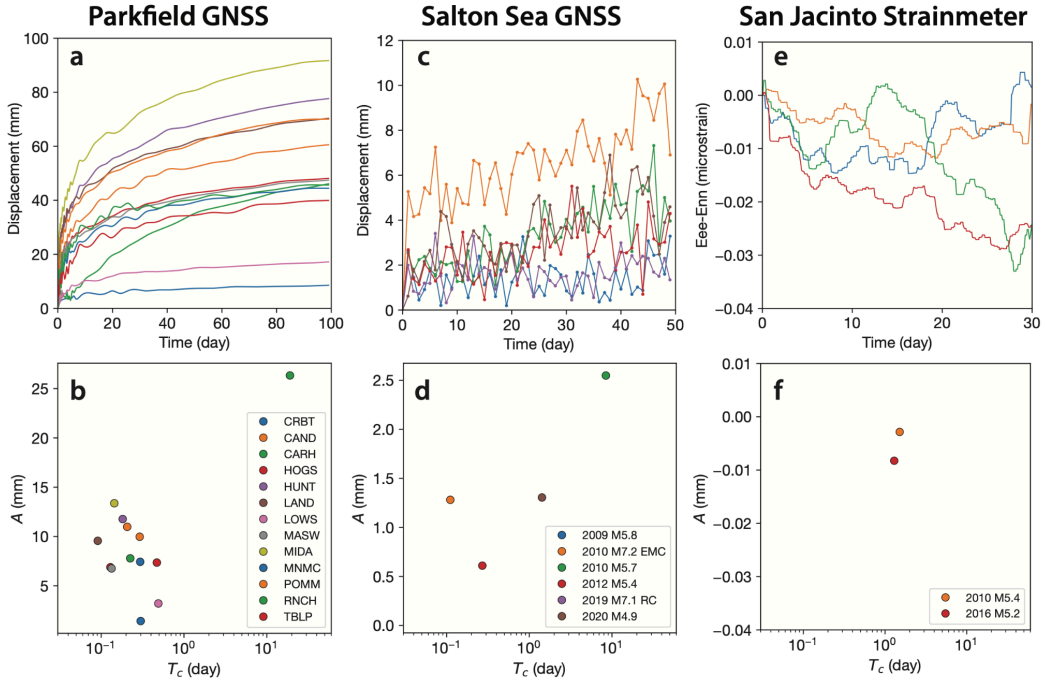

Figure 3. Characterizing GNSS and strainmeter records. GNSS horizontal displacement amplitudes at (a, b) Parkfield and (c, d) Salton Sea, and strain signals at (e, f) San Jacinto fault. (b, d, f) Effective logarithmic amplitude vs timescale for each record. Colors indicate different (a, b) stations or (c–f) triggering events

Results: Repeating Earthquake Analysis

Taira's work has updated CRE catalogs in the Parkfield and San Juan Bautista segments of the San Andreas fault till 2025. We have used the better-quality catalogs for these faults in our initial analysis. For Parkfield, we convert each CRE group into a fault slip history based on the conventional slip-moment relation (Nadeau & Johnson, 1998; Nadeau & McEvilly, 2004) and estimate their effective timescales (Figure 4). We find that the estimated timescales range from 1–100 days, some notably higher than GNSS-based estimates (Figure 3b). This discrepancy may arise from inaccuracy in slip-moment scaling that is calibrated based on steady interseismic measurements. Nonetheless, we observe much smaller timescales around the rupture zone than those further into the lateral creeping areas. Since CRE-based estimates are sensitive to in-situ fault slip, the relative difference clearly points to different temporal behavior and rheological properties, partly corroborating the different estimates observed between GNSS and creepmeters. These results show the promise in probing complex fault processes by leveraging diverse geodetic and seismic observations.

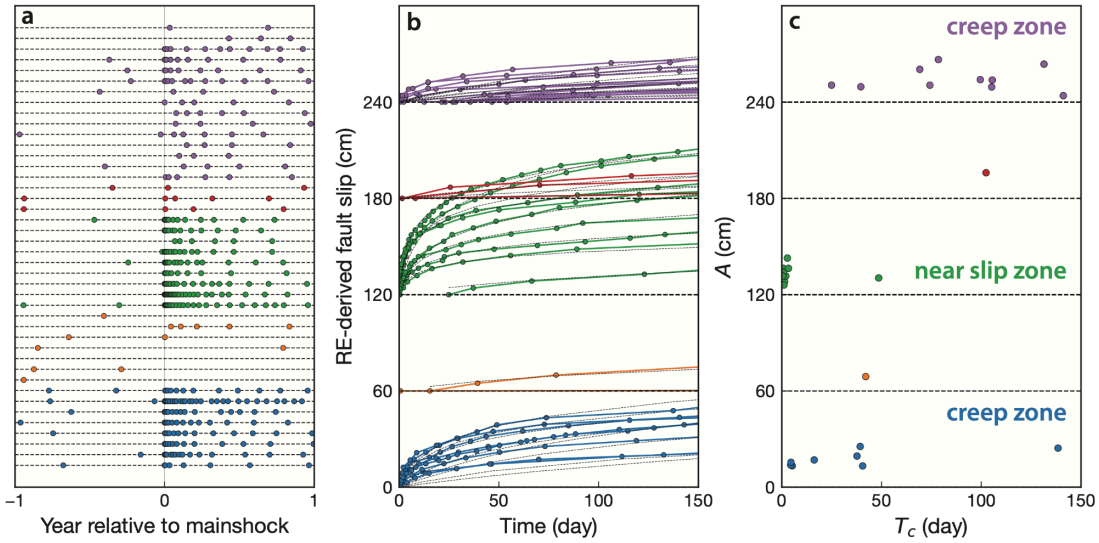

Figure 4. Characterizing fault slip derived from repeating earthquakes. (a) Temporal occurrence of repeating earthquakes near Parkfield. Each line shows one CRE group within different clusters (in colors). (b) Effective postseismic fault slip for each CRE cluster. (c) Effective amplitudes and timescales of CRE fault slip.

Besides updating CREs in Northern California, Taira also improved CRE detection and updated a catalog for part of Southern California (Figure 5). This catalog documents repeating events along the San Jacinto fault zone and others using the SCSN relocated catalog (1981–2018). About 1350 repeating earthquake sequences (M >= 1.0) are identified with a coherence threshold >= 0.95, with a subset of 175 sequences with life spans greater than 1000 days and ~15 pairs having recurrent intervals longer than 10 years. These catalogs reveal distinct CRE behavior: (1) abundant, frequent CREs (CSAF), (2) fewer CREs with longer recurrence interval (SJF, SSGF), and (3) limited or no CREs (SSAF, SHF). While sparse CREs in Southern California make it challenging for high-temporal-resolution kinematic analysis, they will provide unique information that complements our geodetic and physics-based modeling in the future.

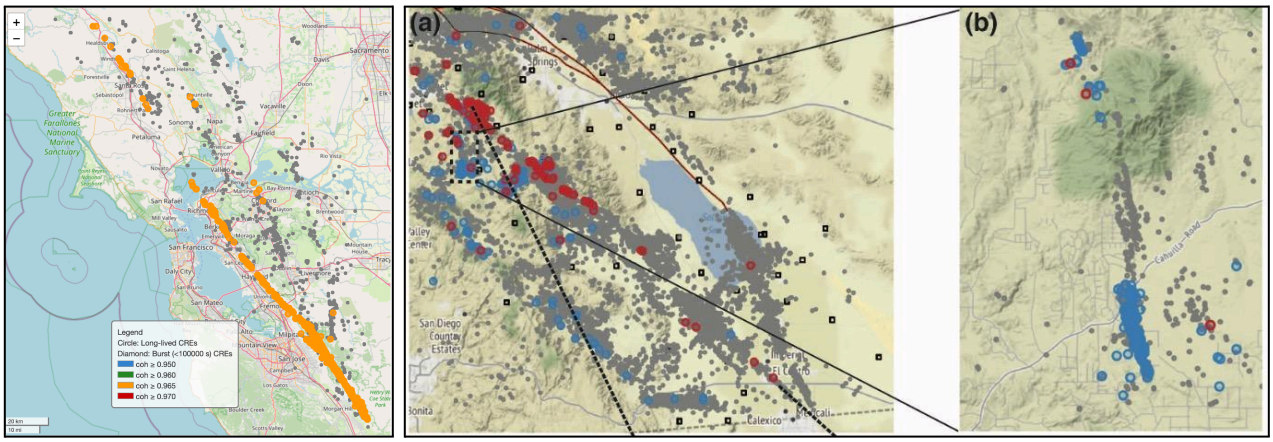

Figure 5. Map view of repeating earthquakes in California. (Left) The Northern California catalog shows events with different coherence thresholds in colors. (Right) The Southern California catalog uses a coherence threshold of 0.95. Gray dots are background events. (a–b) Blue and red circles represent sequences with lifespans of over 100 days and 1000 days, respectively, with an enlarged view around the Cahuilla earthquake swarm.

References

Agnew, D. C. (1986). Strainmeters and tiltmeters. *Reviews of Geophysics*, *24*(3), 579–624. https://doi.org/10.1029/RG024i003p00579

Bakun, W. H., Aagaard, B., Dost, B., Ellsworth, W. L., Hardebeck, J. L., Harris, R. A., et al. (2005). Implications for prediction and hazard assessment from the 2004 Parkfield earthquake. *Nature*, *437*(7061), 969–974. https://doi.org/10.1038/nature04067

Bilham, R, Suszek, N., & Pinkney, S. (2004). California Creepmeters. *Seismological Research Letters*, *75*(4), 481–492. https://doi.org/10.1785/gssrl.75.4.481

Bilham, Roger, & Behr, J. (1992). A 2-layer model for aseismic slip on the Superstition Hills Fault, California. *Bulletin of the Seismological Society of America*, *82*(3), 1223–1235.

Burgmann, R., Schmidt, D., Nadeau, R. M., d'Alessio, M., Fielding, E., Manaker, D., et al. (2000). Earthquake potential along the Northern Hayward fault, California. *Science*, *289*(5482), 1178–1182. https://doi.org/10.1126/science.289.5482.1178

Gittins, D. B., & Hawthorne, J. C. (2022). Are Creep Events Big? Estimations of Along-Strike Rupture Lengths. *Journal of Geophysical Research: Solid Earth*, *127*(1), e2021JB023001. https://doi.org/10.1029/2021JB023001

Gittins, D. B., & Hawthorne, J. C. (2024). Scattered M3–4 Slip Bursts Within Creep Events on the San Andreas Fault. *Journal of Geophysical Research: Solid Earth*, *129*(6), e2023JB028187. https://doi.org/10.1029/2023JB028187

Hauksson, E., Yang, W., & Shearer, P. M. (2012). Waveform relocated earthquake catalog for Southern California (1981 to June 2011). *Bulletin of the Seismological Society of America*, *102*(5), 2239–2244. https://doi.org/10.1785/0120120010

Hawthorne, J. C., Simons, M., & Ampuero, J. P. (2016). Estimates of aseismic slip associated with small earthquakes near San Juan Bautista, CA. *Journal of Geophysical Research: Solid Earth*, *121*(11), 8254–8275. https://doi.org/10.1002/2016JB013120

Inbal, A., Ampuero, J. P., & Avouac, J. P. (2017). Locally and remotely triggered aseismic slip on the central San Jacinto Fault near Anza, CA, from joint inversion of seismicity and strainmeter data. *Journal of Geophysical Research: Solid Earth*, *122*(4), 3033–3061. https://doi.org/10.1002/2016JB013499

Jiang, J., & Lohman, R. B. (2021). Coherence-guided InSAR deformation analysis in the presence of ongoing land surface changes in the Imperial Valley, California. *Remote Sensing of Environment*, *253*, 112160. https://doi.org/10.1016/j.rse.2020.112160

Jiang, J., Bock, Y., & Klein, E. (2021). Coevolving early afterslip and aftershock signatures of a San Andreas fault rupture. *Science Advances*, *7*(15), eabc1606. https://doi.org/10.1126/sciadv.abc1606

Johanson, I. A., Fielding, E. J., Rolandone, F., & Bürgmann, R. (2006). Coseismic and Postseismic Slip of the 2004 Parkfield Earthquake from Space-Geodetic Data. *Bulletin of the Seismological Society of America*, *96*(4B), S269–S282. https://doi.org/10/fjt47d

Johnston, M. J. S., Borcherdt, R. D., Linde, A. T., & Gladwin, M. T. (2006). Continuous Borehole Strain and Pore Pressure in the Near Field of the 28 September 2004 M 6.0 Parkfield, California, Earthquake: Implications for Nucleation, Fault Response, Earthquake Prediction, and Tremor. *Bulletin of the Seismological Society of America*, *96*(4B), S56–S72. https://doi.org/10.1785/0120050822

Jolivet, R., Simons, M., Agram, P. S., Duputel, Z., & Shen, Z. K. (2015). Aseismic slip and seismogenic coupling along the central San Andreas Fault. *Geophysical Research Letters*, *42*(2), 297–306. https://doi.org/10.1002/2014GL062222

Langbein, J., Murray, J. R., & Snyder, H. A. (2006). Coseismic and Initial Postseismic Deformation from the 2004 Parkfield, California, Earthquake, Observed by Global Positioning System, Electronic Distance Meter, Creepmeters, and Borehole Strainmeters. *Bulletin of the Seismological Society of America*, *96*(4B), S304–S320. https://doi.org/10/dnsd9h

Langbein, John, Bilham, R., Snyder, H. A., & Ericksen, T. (2024). *Summary of Creepmeter Data from 1980 to 2020—Measurements Spanning the Hayward, Calaveras, and San Andreas Faults in Northern and Central California* (No. 2024–1011). *Open-File Report*. U.S. Geological Survey. https://doi.org/10.3133/ofr20241011

Lindsey, E. O., Fialko, Y., Bock, Y., Sandwell, D. T., & Bilham, R. (2014). Localized and distributed creep along the southern San Andreas Fault. *Journal of Geophysical Research: Solid Earth*, *119*(10), 7909–7922. https://doi.org/10.1002/2014JB011275

Liu, Y.-K., Ross, Z. E., Cochran, E. S., & Lapusta, N. (2022). A unified perspective of seismicity and fault coupling along the San Andreas Fault. *Science Advances*, *8*(8), eabk1167. https://doi.org/10.1126/sciadv.abk1167

Lohman, R. B., & McGuire, J. J. (2007). Earthquake swarms driven by aseismic creep in the Salton Trough, California. *Journal of Geophysical Research: Solid Earth*, *112*(B4), B04405. https://doi.org/10/c2s6xp

Materna, K., Barbour, A., Jiang, J., & Eneva, M. (2022). Detection of Aseismic Slip and Poroelastic Reservoir Deformation at the North Brawley Geothermal Field From 2009 to 2019. *Journal of Geophysical Research: Solid Earth*, *127*(5), e2021JB023335. https://doi.org/10.1029/2021JB023335

Materna, K., Bürgmann, R., Lindsay, D., Bilham, R., Herring, T., Crowell, B., & Szeliga, W. (2024). Shallow Slow Slip Events in the Imperial Valley With Along-Strike Propagation. *Geophysical Research Letters*, *51*(12), e2023GL108089. https://doi.org/10.1029/2023GL108089

Michel, S., Jolivet, R., Lengliné, O., Gualandi, A., Larochelle, S., & Gardonio, B. (2022). Searching for Transient Slow Slips Along the San Andreas Fault Near Parkfield Using Independent Component Analysis. *Journal of Geophysical Research: Solid Earth*, *127*(6), e2021JB023201. https://doi.org/10.1029/2021JB023201

Murray, J., & Langbein, J. (2006). Slip on the San Andreas Fault at Parkfield, California, over Two Earthquake Cycles, and the Implications for Seismic Hazard. *Bulletin of the Seismological Society of America*, *96*(4B), S283–S303. https://doi.org/10/ddh5s9

Nadeau, R. M., & Johnson, L. R. (1998). Seismological studies at Parkfield VI: Moment release rates and estimates of source parameters for small repeating earthquakes. *Bulletin of the Seismological Society of America*, *88*(3), 790–814. https://doi.org/10.1785/BSSA0880030790

Nadeau, R. M., & McEvilly, T. V. (2004). Periodic Pulsing of Characteristic Microearthquakes on the San Andreas Fault. *Science*, *303*(5655), 220–222. https://doi.org/10.1126/science.1090353

Ross, Z. E., Hauksson, E., & Ben-Zion, Y. (2017). Abundant off-fault seismicity and orthogonal structures in the San Jacinto fault zone. *Science Advances*, *3*(3), e1601946. https://doi.org/10.1126/sciadv.1601946

Ross, Z. E., Trugman, D. T., Hauksson, E., & Peter M. Shearer. (2019). Searching for hidden earthquakes in Southern California. *Science*, *364*(6442), 767–771. https://doi.org/10/gg9pmd

Savage, J. C., Svarc, J. L., & Yu, S.-B. (2005). Postseismic relaxation and transient creep. *Journal of Geophysical Research: Solid Earth*, *110*(B11). https://doi.org/10/bnt65v

Segall, P., & Davis, J. L. (1997). GPS Applications for Geodynamics and Earthquake Studies. *Annual Review of Earth and Planetary Sciences*, *25*(1), 301–336. https://doi.org/10/drcgbk

Shaddox, H. R., Schwartz, S. Y., & Bartlow, N. M. (2021). Afterslip and Spontaneous Aseismic Slip on the Anza Segment of the San Jacinto Fault Zone, Southern California. *Journal of Geophysical Research: Solid Earth*, *126*(6), e2020JB020460. https://doi.org/10.1029/2020JB020460

Sirorattanakul, K., Ross, Z. E., Khoshmanesh, M., Cochran, E. S., Acosta, M., & Avouac, J.-P. (2022). The 2020 Westmorland, California Earthquake Swarm as Aftershocks of a Slow Slip Event Sustained by Fluid Flow. *Journal of Geophysical Research: Solid Earth*, *127*(11), e2022JB024693. https://doi.org/10.1029/2022JB024693

Tymofyeyeva, E., Fialko, Y., Jiang, J., Xu, X., Sandwell, D., Bilham, R., et al. (2019). Slow slip event on the southern San Andreas fault triggered by the 2017 Mw 8.2 Chiapas (Mexico) earthquake. *Journal of Geophysical Research: Solid Earth*, *124*(9), 9956–9975. https://doi.org/10.1029/2018jb016765

Uchida, N., & Bürgmann, R. (2019). Repeating Earthquakes. *Annual Review of Earth and Planetary Sciences*, *47*(1), 305–332. https://doi.org/10.1146/annurev-earth-053018-060119

Vavra, E. J., Fialko, Y., Rockwell, T., Bilham, R., Štěpančíková, P., Stemberk, J., et al. (2024). Characteristic Slow-Slip Events on the Superstition Hills Fault, Southern California. *Geophysical Research Letters*, *51*(12), e2023GL107244. https://doi.org/10.1029/2023GL107244

Waldhauser, F., & Ellsworth, W. L. (2000). A Double-Difference Earthquake Location Algorithm: Method and Application to the Northern Hayward Fault, California. *Bulletin of the Seismological Society of America*, *90*(6), 1353–1368. https://doi.org/10.1785/0120000006

Wei, M., Sandwell, D., & Fialko, Y. (2009). A silent Mw4.7 slip event of October 2006 on the Superstition Hills fault, southern California. *Journal of Geophysical Research: Solid Earth*, *114*(7), B07402. https://doi.org/10.1029/2008JB006135

Wei, M., Liu, Y., Kaneko, Y., McGuire, J. J., & Bilham, R. (2015). Dynamic triggering of creep events in the Salton Trough, Southern California by regional M ≥ 5.4 earthquakes constrained by geodetic observations and numerical simulations. *Earth and Planetary Science Letters*, *427*, 1–10. https://doi.org/10/f7ncpj

Wei, S., Avouac, J.-P., Hudnut, K. W., Donnellan, A., Parker, J. W., Graves, R. W., et al. (2015). The 2012 Brawley swarm triggered by injection-induced aseismic slip. *Earth and Planetary Science Letters*, *422*, 115–125. https://doi.org/10/f7dr4m